

Prediction of Observing Conditions for DES Exposure Scheduling



Eric H. Neilsen, Jr.

Fermi National Accelerator Laboratory
<http://home.fnal.gov/~neilsen>
neilsen@fnal.gov

Dark Energy Survey techniques and surveys

The DES will measure dark energy equation of state parameters using four methods, requiring data from two surveys.

NARROW-FIELD

The narrow-field survey will consist of observations of a small number of fields on a regular cadence.

TYPE Ia SUPERNOVAE

Because the SN Ia technique relies on exposures taken on a regular cadence in order to measure SN light curves, the narrow field survey will be observed at semi-regular intervals, even at the expense of optimal seeing conditions.

WIDE-FIELD

The wide-field survey will consist of biannual observations of a 5000 square degrees on the sky in each filter.

BARYON ACOUSTIC OSCILLATIONS

GALAXY CLUSTERS

WEAK GRAVITATIONAL LENSING

The weak gravitational lensing technique depends on ellipticity measurements on large numbers of galaxies; the wide-field survey is therefore sensitive to seeing conditions.

The DES science observing process

OBSTAC FILLS THE OBSERVING QUEUE

The DES Observing Tactician (ObsTac) fills the observing queue with an initial set of observations appropriate for the start of the night.

ObsTac selects observations based on the need to maintain the observing cadence for the narrow-field survey, the positions of required fields on the sky, an estimate of the seeing based on recent data, and the suitability of the sky brightness (based on the moon altitude and phase) at the required fields for the required filters.

OCS INITIATES THE FIRST EXPOSURE ON THE QUEUE

The observation control system (OCS) removes the first exposure from the queue, and initiates its execution.

OBSTAC REFILLS THE QUEUE

ObsTac adds new exposures to the queue until it reaches the configured duration, taking into account sky and seeing conditions measured previously this night.

EXPOSURE COMPLETED

ObsTac requires an estimate of the seeing to determine whether to observe the narrow or wide-field survey, and an estimate of the sky brightness to determine which pointings and filters are observable.

Sky brightness

REFERENCE SKY BRIGHTNESS DATA

The Sloan Digital Sky Survey (SDSS) photometric telescope (PT) is a 20" telescope used to monitor extinction and calibrate standard stars for the SDSS. The PT collected more than 20,000 sequences of 5 exposures (one in each of the 5 SDSS filters) from 1999 to 2008, over a range of airmasses and moon conditions. These exposures form the reference data set for the sky brightness model considered here.

To model the sky for the DES, model parameters for the moonless sky can be fit to the data set from the Blanco Cosmology Survey (BCS), taken with the same telescope to be used for DES, but the BCS data is insufficient for fitting scattered moonlight or other parameters. Values of these parameters from the PT model are consistent with the BCS data, and will be used as initial estimates.

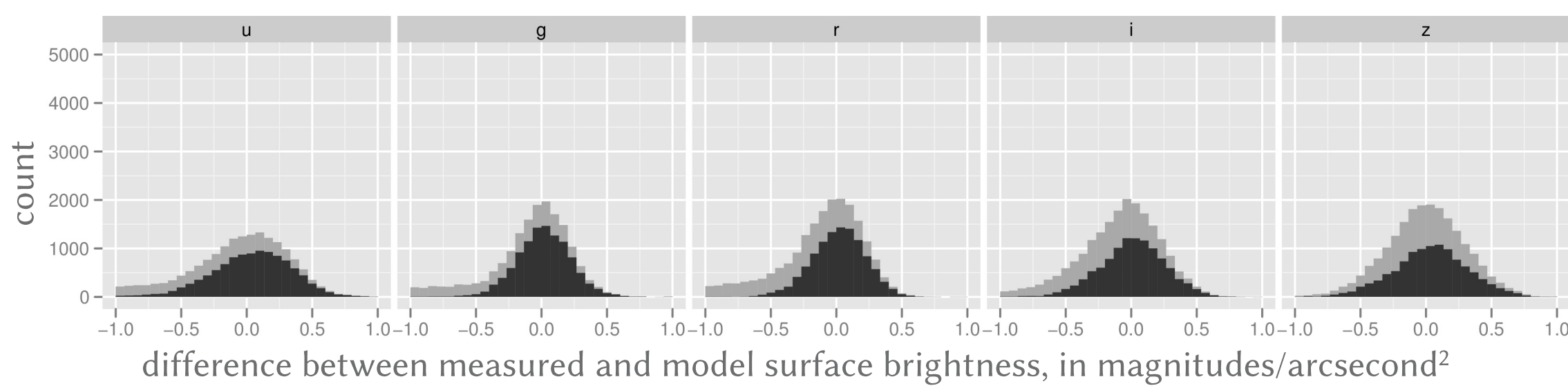
AIRGLOW

This model estimates airglow using the thin spherical shell model of van Rijn (1921). In this model, more flux is seen at higher zenith distances because the line of sight passes through the shell at a shallower angle. The histograms below show the differences (in magnitudes/arcsec²) between a van Rijn airglow model fit to the PT data and the PT data itself. The dark gray portions represent observations taken when the moon was above the horizon; narrow, sharply peaked histograms represent models that fit the data well, while broad and shallow histograms indicate a poor fit to the data.

Simple geometry leads this expression for the surface brightness:

$$m = m_{\text{moon}} + 1.25 \log_{10} \left(1 - \frac{R}{R+h} \sin^2 z \right) + k(X-1)$$

where R is the radius of the Earth and h is the height of the airglow shell. Over the range of zenith distances covered by the SDSS PT data set (and to be covered by DES science observing), the variation of airglow flux is relatively small.



SCATTERING OF MOONLIGHT

Moonlight scattered off atmospheric gases and aerosols is often the dominant source of sky brightness. In addition to depending on the brightness of the moon, the brightness along a line of sight depends on the scattering functions, which are functions of the angle between the moon and the line of sight. The effective extinction is the sum of the extinction between the moon and the scattering particle, and the particle and the observer, so the brightness is a function of both the airmass of the moon and the line of sight.

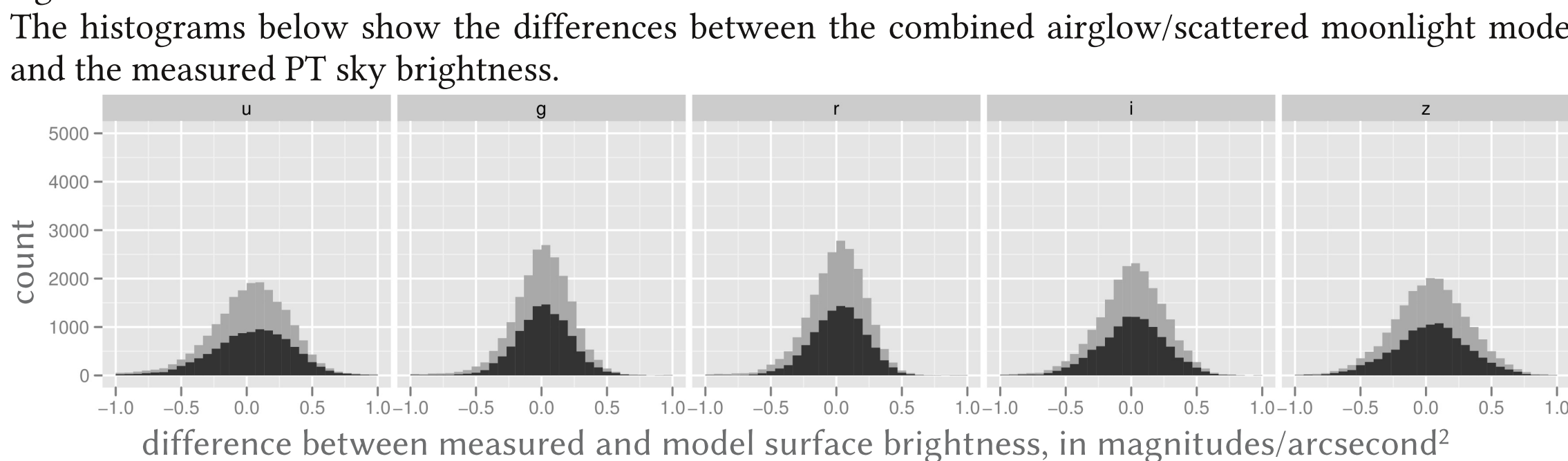
Scattering of moonlight off of atmospheric gases is Rayleigh scattering:

$$f(\rho) = \frac{3}{4}(1 + \cos^2 \rho)$$

where ρ is the scattering angle. Atmospheric aerosols are modeled using the Cornette & Shank (1992) approximation of the Mie scattering function:

$$f(\rho) = \frac{3(1-g^2)}{2(2+g^2)(1+g^2-2g \cos \rho)}$$

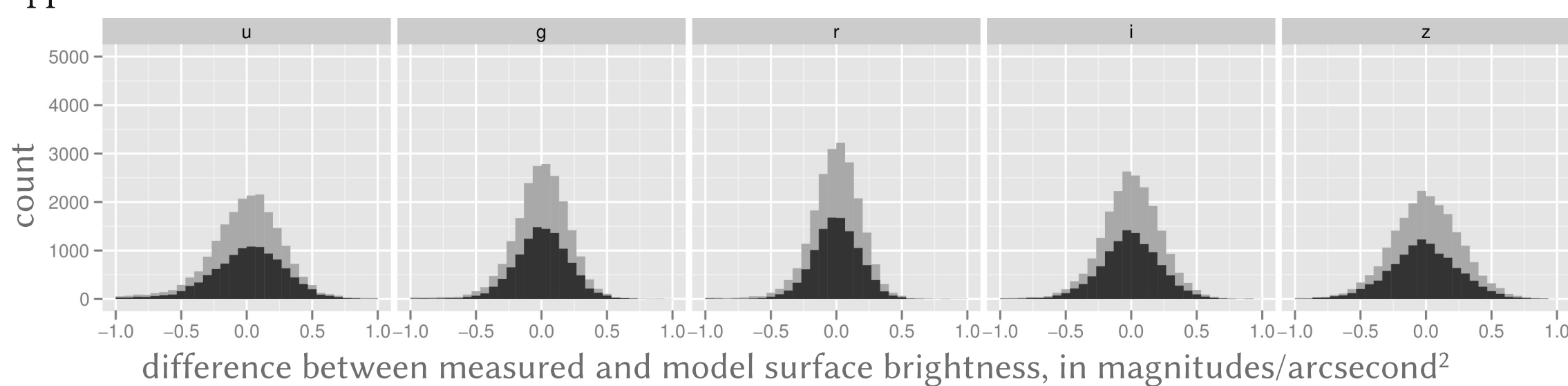
where g is an asymmetry factor.



OTHER SOURCES OF SKY BRIGHTNESS

There are many additional source of sky brightness, including light pollution, unresolved astronomical sources, zodiacal light, gegenschein, and polar aurorae. These are not modeled explicitly. Instead, the offsets from the best fit model of airglow and scattered moonlight are fit to a low order function of airmass, azimuth, time of night, and time of year.

The histograms below show the remaining difference between model and measured value after the application of these offsets.



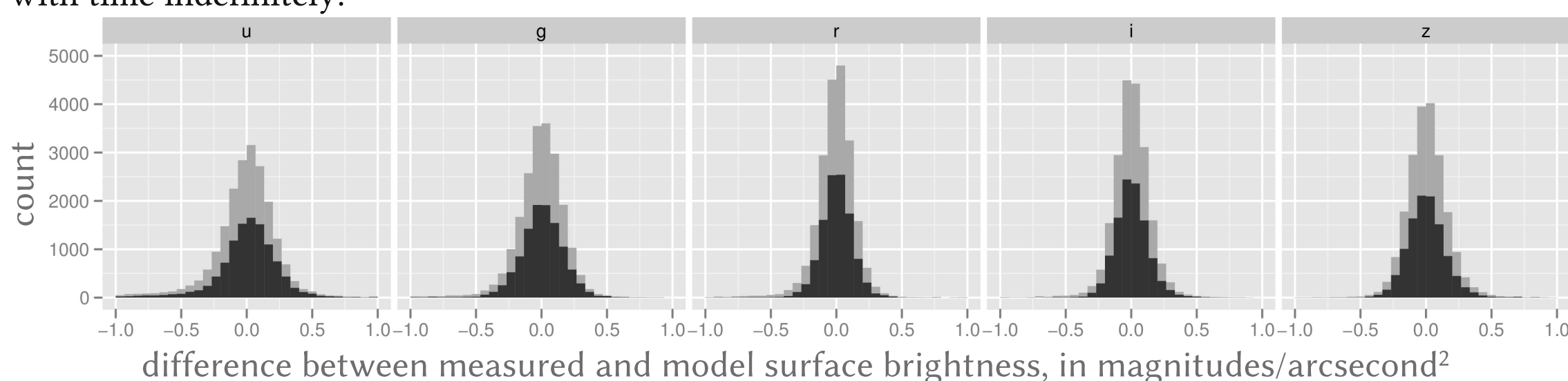
MODEL OFFSETS AS AN AUTO-REGRESSIVE TIME SERIES

Even after fits to obvious astronomical and positional parameters have been subtracted, significant residuals remain. These residuals are strongly correlated in time, suggesting that a good estimate of the offset from the model in the near future is the offset from the model in the recent past. An auto-regressive model, in which the offset at time t is the weighted mean of the global mean and some number of previous time steps, is one way of modeling such a system. For this model, the mean offset is zero and a linear combination of the two previous time steps accounts for most temporal correlation. In the r filter, for example, the best fit AR(2) model for the offsets is:

$$\Delta D_t = 0.70 \Delta D_{t-1} + 0.13 \Delta D_{t-2} + e_t$$

where e_t follows a normal distribution with variance 0.013, resulting in an uncertainty of 0.11 mag/arcsec². Over time, the uncertainty relative to the global model tends to 0.17 mag/arcsec² rather than increasing with time indefinitely.

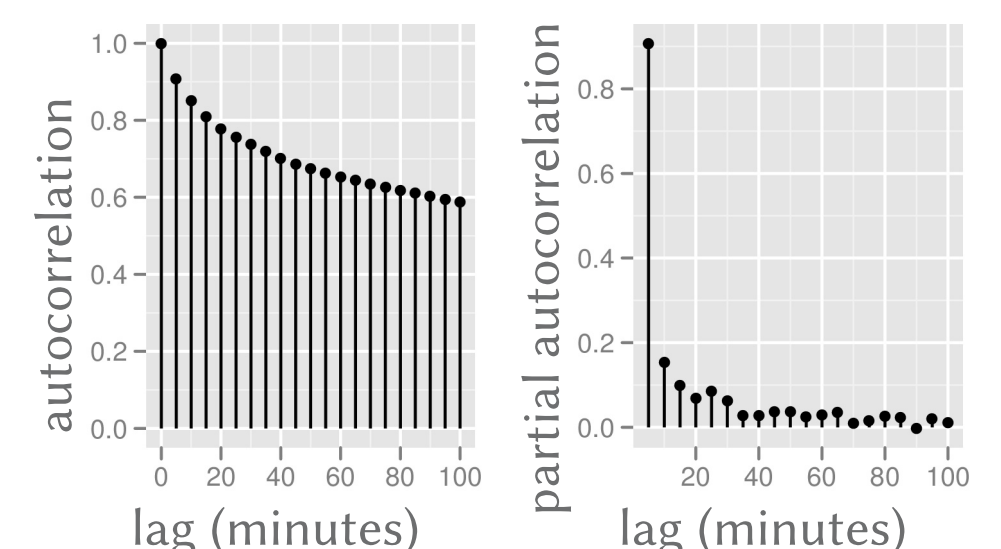
The auto-regressive model is a generalization of a simple random walk. Unlike the random walk, however, the expected distance from the mean does not increase indefinitely with time. The AR model is therefore more suitable when it might be used, for example, to simulate data to test observing strategy.



Variation of seeing with time

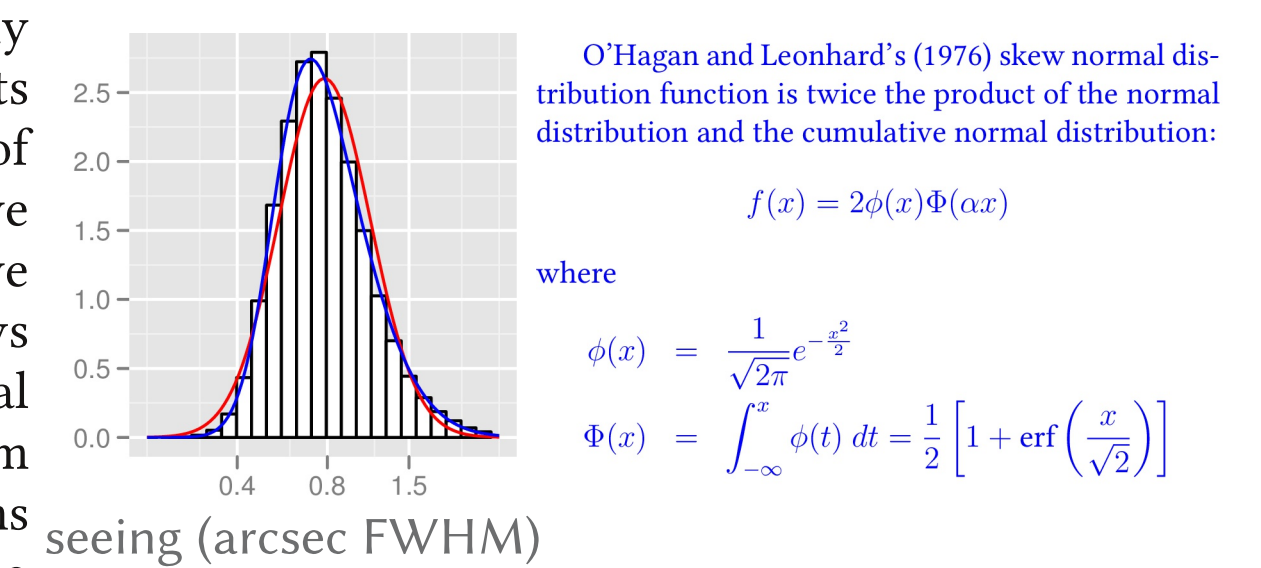
SEEING AUTOCORRELATION

The autocorrelation function of the seeing, as measured from DIMM data from the CTIO archive, decays gradually in time, while the partial autocorrelation function drops to near zero after the first few time steps. This pair of features suggests that the series can be modeled as an auto-regressive process, in which the value at any given time is the weighted average of the global mean, the values of a small number of previous steps, and a random value.



SEEING DISTRIBUTION

Because auto-regressive processes produce normally distributed values, the set of FWHM measurements needs to be transformed to a normally distributed set of values. The FWHM distribution has a strong positive skew, and even the log distribution retains some positive skewness; the red line on the seeing histogram shows the best fit log-normal distribution. A log-skew-normal fit, shown in blue, provides a reasonable match. From this fit, I derive a monotonic function that transforms the measured distribution of FWHM values into a normal distribution of values, s_t .



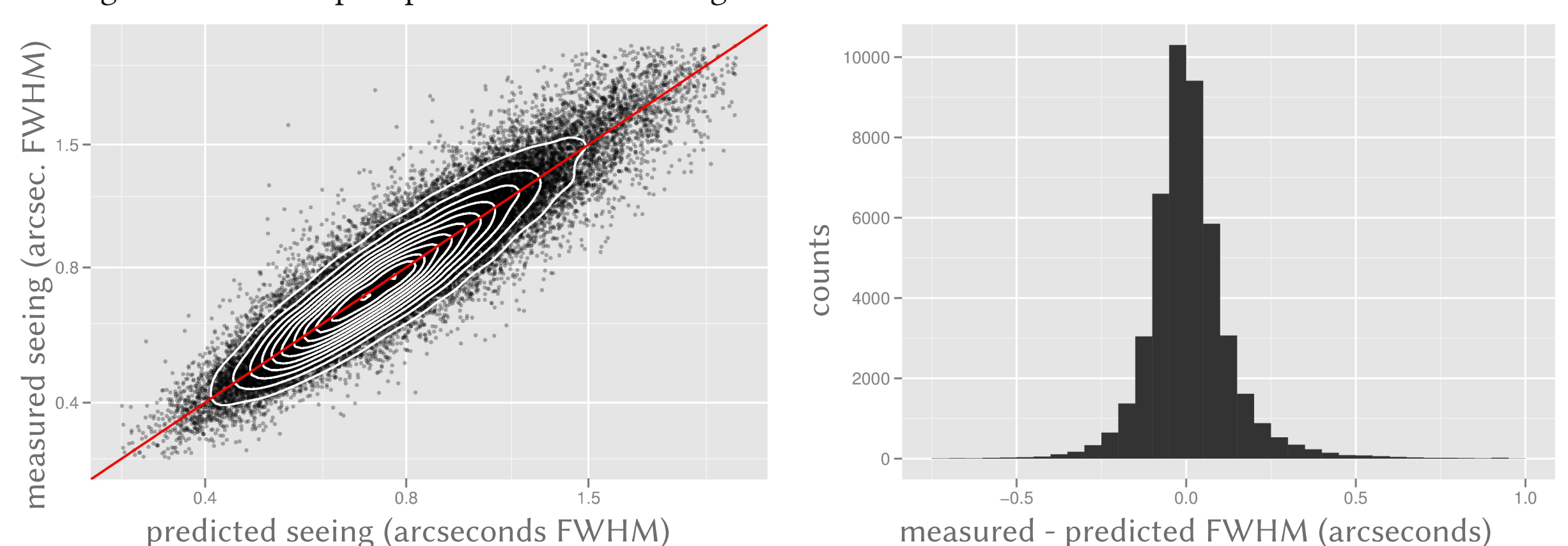
SEEING VARIATIONS AS AN AUTO-REGRESSIVE TIME SERIES

For the transformed value s_t , a good auto-regressive function for s_t is

$$s_t = 0.48s_{t-1\text{day}} + 0.13s_{t-10\text{min}} + 0.80s_{t-5\text{min}} + e_t$$

where e_t is normally distributed with a standard deviation of 0.38. The value $s=0.0$ corresponds to a PSF with FWHM=0.76" and $s=0.38$ corresponds to FWHM=0.87", indicating variations of order 0.1" are introduced in each 5 minute time interval. Indeed, the differences between predictions made with this model and measured values have a standard deviation of 0.13". The median absolute deviation is only 0.06" and distribution has a high kurtosis of 17.7; small and large deviations are significantly more common than would be predicted by a normal distribution.

The figures below compare predictions made using this model to measured values.



Future work

These models are being incorporated into ObsTac, where they will be used for two purposes. First, they will be used during observing for selection of observations, as described above. A second major use for these models is in the simulation of the surveys that we use to optimize survey strategy.

Funding for the DES Projects has been provided by the U.S. Department of Energy, the U.S. National Science Foundation, the Ministry of Science and Education of Spain, the Science and Technology Facilities Council of the United Kingdom, the Higher Education Funding Council for England, the National Center for Supercomputing Applications at the University of Illinois at Urbana-Champaign, the Kavli Institute of Cosmological Physics at the University of Chicago, Financiadora de Estudos e Projetos, Fundação Carlos Chagas Filho de Amparo à Pesquisa do Estado do Rio de Janeiro, Conselho Nacional de Desenvolvimento Científico e Tecnológico and the Ministério da Ciência e Tecnologia, the Deutsche Forschungsgemeinschaft and the Collaborating Institutions in the Dark Energy Survey. The Collaborating Institutions are Argonne National Laboratories, the University of California at Santa Cruz, the University of Cambridge, Centro de Investigaciones Energéticas, Medioambientales y Tecnológicas-Madrid, the University of Chicago, University College London, DES-Brazil, Fermilab, the University of Edinburgh, the University of Illinois at Urbana-Champaign, the Institut de Ciències de l'Espanya (IEEC/CSIC), the Institut de Física d'Àltes Energies, the Lawrence Berkeley National Laboratory, the Ludwig-Maximilians Universität and the associated Excellence Cluster Universe, the University of Michigan, the National Optical Astronomy Observatory, the University of Nottingham, the Ohio State University, the University of Pennsylvania, the University of Portsmouth, SLAC, Stanford University, the University of Sussex, and Texas A&M University. Fermilab is operated by Fermi Research Alliance, LLC under Contract No. De-AC02-07CH11359 with the United States Department of Energy.

